Schulz–Flory oligomerisation of ethylene by the binuclear nickel(II) complex Ni_2Cl_4[*cis,trans,cis*-1,2,3,4-tetrakis-(diphenylphosphino)cyclobutane]

Claudio Bianchini,*[a] Luca Gonsalvi,[a] Werner Oberhauser,[a] David Sémeril,[a] Peter Brüggeller[b] and Rene Gutmann[b]

[a] *Istituto di Chimica dei Composti Organometallici, ICCOM-CNR, Area della Ricerca di Firenze, Via Madonna del Piano snc, 50019 Sesto Fiorentino (Firenze), Italy.*
E-mail: cbianchini@iccom.cnr.it
[b] *Institut für Allgemeine, Anorganische und Theoretische Chemie der Universität Innsbruck, Innrain 52a, Innsbruck, Austria*

The binuclear nickel(II) complex Ni_2Cl_4(*cyclo*-tetraphos) (*cyclo*-tetraphos = *cis,trans,cis*-1,2,3,4-tetrakis-(diphenylphosphino)cyclobutane) forms, upon activation with MAO, an effective and robust catalyst for the oligomerisation of ethylene to Schulz–Flory distributions of C_4–C_{14} olefins with a mechanism where both chain transfer and chain propagation are first order in ethylene.

Introduction

The majority of single-site nickel catalysts for the homogeneous oligomerisation of ethylene comprises chelating bidentate ligands with at least one hard donor atom bound either to Ni^{II} compounds, commonly bis-halides, or to Ni^0 compounds capable of forming Ni^{II}–H species upon oxidative addition. In the former case, common activators to initiate the catalytic cycle are methyl alumoxane (MAO) or aluminium alkyls. Anionic and neutral P,O ligands such as those employed in the SHOP process,[1] yielding linear α-olefins, still generate the most efficient industrial catalysts, yet interesting results have been obtained with α-diimines,[2] pyridinimines,[3] iminophosphines,[4] iminophosphoranes,[5] phosphinidines[6] and diamines.[7] Ethylene oligomerisation Ni^{II} catalysts with diphosphine ligands bearing sp^3-hybridised phosphorus donors are still a rarity and generally produce low molecular weight products in low yield due to fast termination by β-H transfer.[8]

In order to disfavour chain transfer over chain propagation in ethylene oligomerisation and polymerisation reactions catalysed by diphosphine–Ni^{II} complexes, some successful strategies have been recently developed, which involve: (i) decrease of the flexibility of the metal-ligand assembly; (ii) increase of the steric protection in the axial positions relative to the (P–P)Ni coordination plane; (iii) decrease of the ligand nucleophilicity (hence of the metal basicity). When all these three conditions are efficiently achieved as in the paradigmatic cases of diphosphinidenecyclobutenes (**A**),[6c] 1,4-diphospha-1,3-butadienes (**B**)[6b] or bis(diarylphosphino)methylamines (**C**) (Chart 1),[9a,b] chain transfer is so retarded that the resulting Ni^{II} complexes become active polymerisation catalysts for high molecular weight polyethylene. For Ni complexes of 1,3-diphosphapropene, it was shown that catalyst stability and activity was increased through the distribution of three electrons in a η^3-1,3-diphosphaallyl chelate fashion.[9c]

Partial accomplishment of the conditions detailed above may result in selective oligomerisation catalysts as is the case of the 1,2-bis(diarylphosphino)methane ligands **D** which are polymerisation catalysts for R = Pr^i, CF_3, and oligomerisation catalysts for R = Me (Chart 1).[9b]

The presence of two or more CH_2 spacers between the P(aryl)₂ groups, as in 1,2-bis(diarylphosphino)ethane or 1,2-bis(diarylphosphino)propane, makes the corresponding Ni^{II}-diphosphine complexes inefficient for both oligomerisation and polymerisation of ethylene, irrespective of the number and size of the aryl substituents.[9b]

In previous works, we have reported that the tetraphosphine *cis,trans,cis*-1,2,3,4-tetrakis-(diphenylphosphino)cyclobutane (*cyclo*-tetraphos) (Chart 2) generates Pd^{II} catalysts which are more efficient and selective than analogous catalysts with traditional 1,2-bis(diphenylphosphino) ligands.[10,11]

In particular, *cyclo*-tetraphos forms a Pd^{II} catalyst for the alternating CO/ethylene copolymerisation that is from three to four times more active than the analogous catalyst with 1,2-bis(diphenylphosphino)ethane (dppe).[10] The same *cyclo*-tetraphos catalyst is much more selective in the oxidative
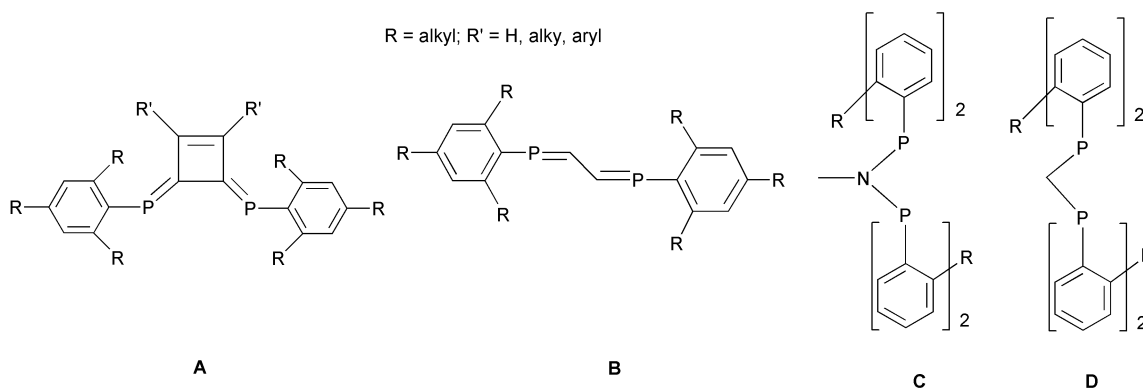
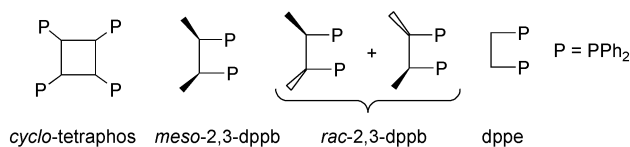R = alkyl; R' = H, alky, aryl

Chart 1

Chart 2

carbonylation of styrene to methyl cinnamate than similar catalysts with dppe, *meso*-2,3-bis(diphenylphosphino) butane (*meso*-dppb) or *rac*-2,3-bis(diphenylphosphino) butane (*rac*-dppb) (Chart 2).[11]

In both reactions investigated, the better performance of the *cyclo*-tetraphos catalysts was ascribed to the lower propensity to β-H transfer of the rigid structure of the Pd$_2$-cyclotetraphos assembly in which the two metalla-rings adopt an envelope conformation and each phosphorus bears one axial and one equatorial phenyl group.[12]

X = monodentate ligand
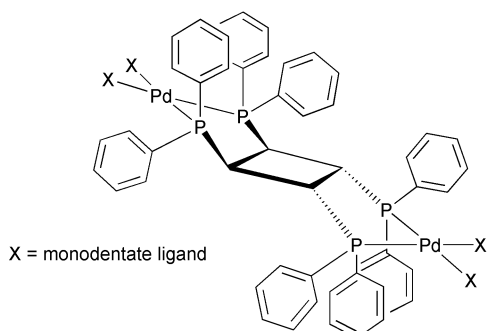
These favourable structural features of palladium complexes with *cyclo*-tetraphos prompted us to investigate the potential of this ligand in ethylene oligomerisation by nickel(II) catalysis. The catalytic performance of related nickel precursors stabilised by *meso*-dppb, *rac*-dppb and dppe was investigated under comparable conditions. The results obtained have confirmed the peculiar properties of *cyclo*-tetraphos, which in conjunction with nickel(II) bis-chloride and MAO, provides an effective and robust catalyst for the oligomerisation of ethylene to Schulz–Flory distributions of linear C_4–C_{14} olefins.

Results and discussion

Synthesis and characterisation of the nickel(II) precursors

The Ni^{II} complexes used in this study as catalyst precursors for the oligomerisation of ethylene are shown in Chart 3.
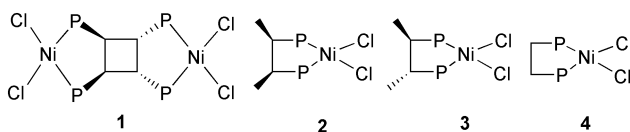

Chart 3

The plain reaction of NiCl$_2$·6H$_2$O in ethanol with an equivalent amount of each ligand dissolved in CH$_2$Cl$_2$ gave in all cases diamagnetic red–orange crystals in fairly good yields. Recrystallisation from appropriate solvents provided single crystals of **1**·2DMF, **2**·0.5toluene and **3** suitable for X-ray diffraction analyses. ORTEP drawings are presented in Fig. 1–3, while selected bond distances and angles are reported in Table 1.

All three structures exhibit a square planar coordination geometry around the nickel(II) centres. The P–Ni–P bite angles, 86.45(11)° for **1**, 85.52(5)° for **2**, and 86.82(3)° for **3**, are comparable to each other and lie in the typical range for five-membered chelate rings. The deviations of the Ni atom from the coordination plane, defined by the atoms Cl1, Cl2, P1, P2, are 0.0884 Å for the centrosymmetric binuclear complex **1**,
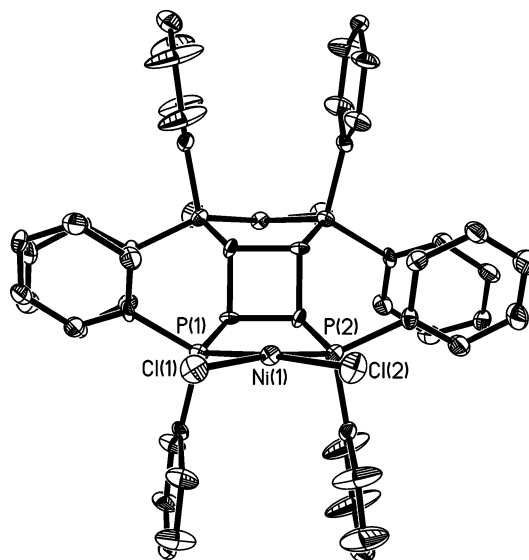

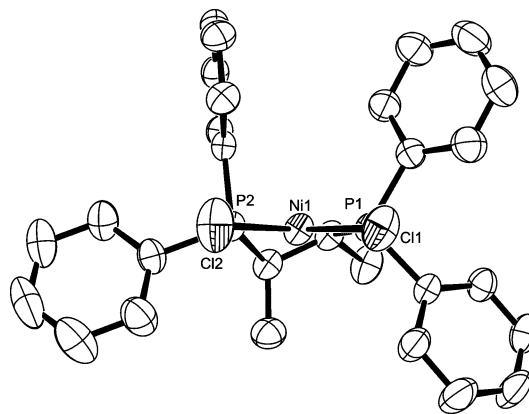**Fig. 1** X-Ray crystal structure of **1**, solvent omitted for clarity.

Fig. 2 X-Ray crystal structure of **2**, solvent omitted for clarity.
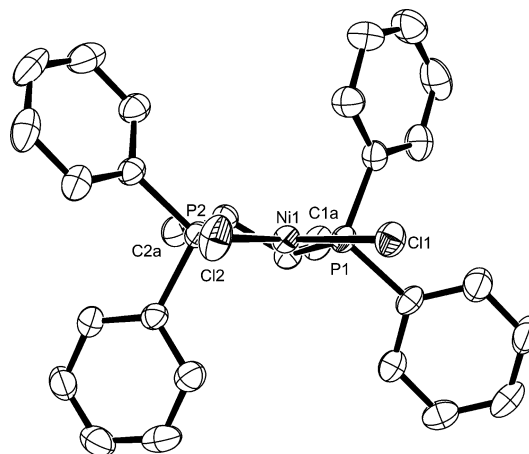
Fig. 3 X-Ray crystal structure of **3**.

0.0178 Å for the *meso*-dppb complex **2** and 0.0224 Å for the *rac*-dppb complex **3**.

The bridging carbon atoms C1 and C2 deviate from the ideal coordination plane, defined by Cl1, Cl2, P1, P2, by 0,6125 Å for **1** and by −0.1741 and −0.8387 Å for **2**. Compound **3** exhibits a twisted conformation as it was previously determined for the dppe complex **4**.[8] Consistently, the carbon atoms C1 and C2 deviate in opposite directions (0.3862 and −0.3691 Å) from the coordination plane. It is worth mentioning that the Flack parameter of −0.011(9) clearly indicates the presence of the pure NiCl$_2$(*R*,*R*-2,3-dppb) enantiomer in the crystal of **3**. Unlike **2** and **3**, the binuclear complex **1** exhibits an envelope conformation of the five-membered rings, which defines two

conformationally rigid, axial phenyl-groups, belonging to the same asymmetric unit and located at the same side of the coordination plane, which anticipates an efficient steric protection of one axial coordination site in square-planar Ni-*cyclo*-tetraphos moieties. Consistently, the distances of the phenyl *ipso*-carbon atoms from the coordination plane (**1** −1.7686(2), −1.8067(2), 0.9150(2), 0.7550(2) Å; **2**: −1.6196(17), −1.7564(15), 1.2708 (20), 0.6361(24) Å; **3**: −1.6760(1), −1.2337(1), 1.6053(1), 1.2337(1) Å) show unequivocally that only **1** contains two axial phenyl groups, the other two being equatorial. Complex **2** contains one pseudoaxial and three pseudoequatorial phenyl groups, while all phenyl groups are pseudoequatorial in **3**.

The room-temperature $^{31}P\{^1H\}$ NMR spectra in CDCl$_3$ show singlets at δ 72.52 (**1**), 60.8 (**2**) and 59.09 (**3**). Complex **1** is stereochemically rigid on the NMR timescale, while **2** is fluxional. Indeed, chelate ring flipping in the *meso*-complex is quite rapid to interchange axial and equatorial CMe groups so that a *pseudo*-symmetry plane makes the phosphorus and methyl groups magnetically equivalent down to −78 °C. Below this temperature, the dynamic process is frozen out and the molecule, like in the solid state, loses any symmetry (AB pattern with doublets at δ 62.10 and 65.10, J_{PP} = 79.2 Hz). At the coalescence (−65 °C), a $\Delta G_c\ddagger$ value of 9.9(1) kcal mol^{-1} was calculated. The presence of a C_2 axis in the *rac* isomer **3** does not allow one to estimate its molecular flexibility by variable-temperature NMR spectroscopy. However, the presence of CMe groups with opposite configuration should make the metalla-ring more rigid than in **2** and much more rigid than in the dppe derivative **4** in which the Ni(dppe) metalla-ring rapidly interconverts from one chiral twisted (δ–λ) conformation to the other.[14] The metalla-ring conformation affects, by symmetry, the spatial distributions of the phenyl substituents on the phosphorus donors so that in the *cyclo*-tetraphos complex the two axial phenyl groups are located on the same side of the

PNiP plane, whereas they reside on opposite sides in the chiral *rac*-dppb conformation. In terms of the well-known "quadrant effect",[15] this means that the steric crowding provided by the phenyl groups is concentrated on one side of the PNiP plane in the *cyclo*-tetraphos complex, whereas it is diagonal with respect to the PNiP plane in the dppe and *rac*-dppb derivatives. The situation for **2** might be intermediate, with a prevalence for two axial and two equatorial phenyl groups in the fast exchange solution regime.

Oligomerisation reactions

Complexes **1**–**4**, in combination with the activator MAO (methyl alumoxane), were evaluated as catalysts for the oligomerisation of ethylene in toluene solution. Table 2 reports on the results of reactions carried out under various experimental conditions. In all cases the addition of ethylene resulted in a rapid exothermic event, indicative of no induction period. In principle this immediate exotherm may affect the oligomerisation results, however in this case the effect appears to be negligible as shown by the experiments carried out at ethylene pressure ranging from 4 to 26.6 bar, indicating almost linear correlation between TOF and ethylene pressure (*vide infra*). Initially all catalysts were tested at 14.3 bar C$_2$H$_4$ pressure and 20 °C for 30 min, with 200 equiv. of MAO both as co-catalyst and reactor scavenger. Catalyst activities [mol of ethylene converted (mol of Ni × h)$^{-1}$] were calculated from the GC readings. Since only traces of hexenes and octenes were produced by **4**, the activity of this precursor was estimated on the basis of the overall butene products in both liquid and gaseous phases.

The *cyclo*-tetraphos catalyst showed the highest activity with a turnover frequency (TOF) of 42700 mol ethylene converted (mol Ni)$^{-1}$ h^{-1} yielding C$_4$–C$_{14}$ olefins with a Schulz–Flory distribution (entry 1).[16] No appreciable formation of either odd carbon oligomers or saturated hydrocarbons was observed, while extensive isomerisation to internal olefins, predominantly with *E* configuration, occurred (*vide infra*). The *meso*-dppb (entry 2) and *rac*-dppb (entry 3) complexes were less active than the *cyclo*-tetraphos complex and surprisingly produced predominantly butenes as indicated by the low α value. The dppe catalyst gave almost exclusively butenes in very low yield (entry 4). This result is not completely unexpected as Wass and coworkers have recently reported that 1,2-bis(diarylphosphino)-ethane ligands, in conjunction with Ni(cod)$_2$ (cod = cyclohexa-1,5-diene) and H(Et$_2$O)B[3,5-C$_6$H$_3$(CF$_3$)$_2$]$_4$, do not oligomerise ethylene, even in the presence of bulky alkyl substituents on the aryl groups.[9b]

Increasing the pressure to 28.6 bar gave higher TOFs for all precursors (entries 5–7), except for **4** (entry 8), which apparently generates an unstable catalyst with a short lifetime (see also entry 12). Remarkably, the activity of the other catalysts

Table 1 Selected bond lengths (Å) and angles (°) for complexes **1**·2DMF, **2**·0.5toluene and **3**

	1·DMF	**2·0.5toluene**	**3**
Ni(1)–P(1)	2.162(3)	2.1656(12)	2.1350(8)
Ni(1)–P(2)	2.152(3)	2.1451(13)	2.1542(8)
Ni(1)–Cl(1)	2.210(3)	2.2061(13)	2.2115(8)
Ni(1)–Cl(2)	2.183(3)	2.1826(13)	2.1783(8)
P(1)–Ni(1)–P(2)	86.45(11)	85.52(5)	86.82(3)
Cl(1)–Ni(1)–Cl(2)	93.97(12)	94.64(5)	95.00(3)
Cl(1)–Ni(1)–P(2)	172.85(13)	175.06(4)	174.46(3)
Cl(1)–Ni(1)–P(1)	90.06(12)	90.01(5)	88.16(3)
Cl(2)–Ni(1)–P(1)	173.21(12)	174.36(3)	176.77(3)
Cl(2)–Ni(1)–P(2)	88.93(12)	89.71(5)	89.99(3)

Table 2 Oligomerisation of ethylene catalysed by Ni$_2$Cl$_4$(*cyclo*-tetraphos)/MAO and NiCl$_2$(P–P)/MAO[a]

Run	Precursor	P–P	Pressure/bar	Time/min	TOF[b]/10^{-4}	α^c	β^d
1	**1**	*cyclo*-tetraphos	14.3	30	4.27	0.250	3.0
2	**2**	*meso*-dppb	14.3	30	2.59	0.074	12.5
3	**3**	*rac*-dppb	14.3	30	3.52	0.057	16.5
4	**4**	dppe	14.3	30	0.14	*d*	*d*
5	**1**	*cyclo*-tetraphos	28.6	30	7.80	0.244	3.1
6	**2**	*meso*-dppb	28.6	30	5.09	0.072	13.0
7	**3**	*rac*-dppb	28.6	30	5.57	0.063	14.9
8	**4**	dppe	28.6	30	0.15	*d*	*d*
9	**1**	*cyclo*-tetraphos	14.3	60	4.17	0.236	3.2
10	**2**	*meso*-dppb	14.3	60	1.92	0.080	11.5
11	**3**	*rac*-dppb	14.3	60	1.98	0.042	22.8
12	**4**	dppe	14.3	60	0.08	*d*	*d*

[a] Catalyst (12 µmol); MAO (200 equiv.); toluene (100 mL); 20 °C; 1500 rpm. [b] Mol of C$_2$H$_4$ converted (mol of Ni)$^{-1}$ h^{-1}, average values from at least three runs determined by GC at appropriate temperatures. [c] Schulz–Flory parameters: a = mol C$_{n+2}$/mol C$_n$; β = (1 − a)/a. [d] Not calculated.
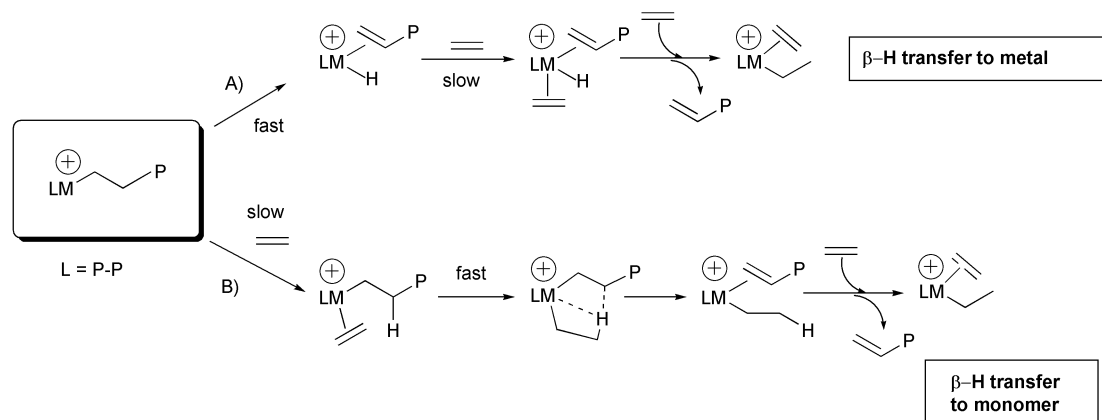
Scheme 1

Table 3 Oligomerisation of ethylene catalysed by Ni_2Cl_4(*cyclo*-tetraphos)/MAO. [a] Dependence on C_2H_4 pressure and reaction time

run	Pressure/bar	Time/min	$TOF^{b}/10^{-4}$	α^{c}	β^{c}
1	4.0	15	1.78	0.298	2.3
2	4.0	30	1.74	0.271	2.7
3	9.6	15	3.18	0.227	3.4
4	9.6	30	3.13	0.231	3.3
5	14.3	15	4.32	0.227	3.4
6	14.3	30	4.27	0.250	3.0
7	14.3	60	4.17	0.226	3.4
8	28.6	30	7.80	0.244	3.1
9	28.6	60	7.75	0.233	3.3

[a] Catalyst (12 μmol); MAO (200 equiv.); toluene (100 mL); 20 °C; 1500 rpm. [b] Mol of C_2H_4 converted (mol of Ni)$^{-1}$ h^{-1} average values from at least three runs. [c] Schulz–Flory parameters: $\alpha = $ mol C_{n+2}/mol C_n; $\beta = (1 - \alpha)/\alpha$.

increased linearly with the C_2H_4 pressure. The highest TOF (78000) was again exhibited by precursor **1** (entry 5).

Increasing the reaction time to 60 min, keeping a constant ethylene pressure of 14.3 bar, gave a surprising result: the TOF of the *cyclo*-tetraphos catalyst did not significantly vary with respect to the 30 min value (entry 9), whereas the TOFs of the *meso*-dppb and *rac*-dppb catalysts decreased by *ca.* one half (entries 10–11). Apparently, only **1** generates a stable catalyst under the present experimental conditions.

For this reason, all further studies were carried out on oligomerisation reactions catalysed by **1**. Table 3 shows the effects of pressure and reaction time on the oligomerisation activity of the *cyclo*-tetraphos catalyst.

Notably, the TOF did not vary with time, irrespective of the pressure, which confirms the excellent stability of the *cyclo*-tetraphos catalyst system. Reactions in the C_2H_4 pressure range from 4.0 to 28.6 bar showed a linear dependence of activity with the pressure, while the α value, which represents the probability of chain transfer (rate of propagation/(rate of propagation + rate of chain transfer)),[16a,b] was independent of the pressure. Therefore, both the propagation and chain transfer rates are first order in ethylene.[17]

The α factor did not change with time, which rules out the occurrence of reincorporation of olefin products into oligomers made later in the reaction.[17a,d] Consistently, the oligomerisation of ethylene with **1** (4.0 bar C_2H_4, 60 min), carried out in the presence of an excess of 1-undecene, did not give any odd-carbon oligomer.

Accurate analyses of the hexene fractions obtained from runs at 28.6 bar for 30 and 60 min showed the prevalent formation of internal olefins with *E* structure. In particular, the reactions gave the following distributions: 30 min: hex-1-ene 52%, *E*-hex-2-ene 19%, *Z*-hex-2-ene 8%, *E*-hex-3-ene 15%, *Z*-hex-3-ene 6%; 60 min: hex-1-ene 40%, *E*-hex-2-ene 22%, *Z*-hex-2-ene 10%,

E-hex-3-ene 25%, *Z*-hex-3-ene 3%. Neither branched olefin (*e.g.* methylpentene) nor hexane were formed. The absence of saturated hydrocarbon products ruled out the occurrence of termination by chain transfer to aluminium.[18]

Mechanistic considerations

The nature and statistical distribution of the olefins produced by the precursors **1**, **2** and **3** are consistent with a standard oligomerisation mechanism involving (i) nickel–alkyl initiators obtained by action of MAO on the dichloride precursors; (ii) propagation by migratory insertion of Ni(alkyl)(ethylene) (Cossee–Arlmann); (iii) termination by chain transfer.[17a,b]

In the reactions catalysed by **1**, the rates of propagation and chain transfer do not differ remarkably from each other under the experimental conditions investigated, the β parameter ($\beta = r_{transfer}/r_{propagation}$) being close to 3 in all runs. In contrast, chain transfer largely prevails over propagation for the reactions catalysed by **2** or **3** (β varies from 12 to 22 in fact). For late transition-metal ethylene oligomerisation catalysts, chain transfer generally occurs by β-hydrogen transfer to give *a*-olefins. Two mechanisms are commonly proposed to account for chain-transfer: path **A** involves an associative displacement step following β-hydrogen transfer to the metal; path **B** proceeds *via* β-H transfer to monomer, *i.e.* the β-hydrogen is directly transferred to the incoming monomer with no formation of metal hydride (Scheme 1). Since both chain growth and chain transfer are first-order in monomer concentration, the rate limiting step involves monomer uptake in either mechanism.

On the basis of the experimental evidence accumulated during this work, it is not possible to discriminate between these two chain-transfer mechanisms, which are kinetically indistinguishable. In view of the effective isomerisation of *a*-olefins to internal olefins, however, β-H transfer to the metal does take place. Once formed, Ni–H may form both primary and secondary Ni–alkyl upon insertion of *a*-olefins (Scheme 2).
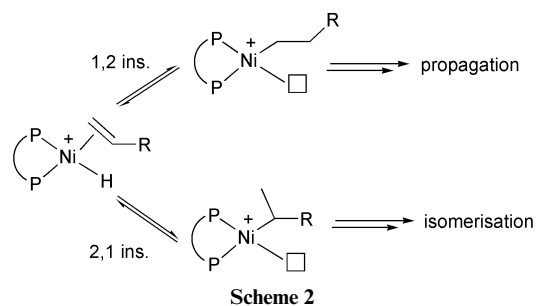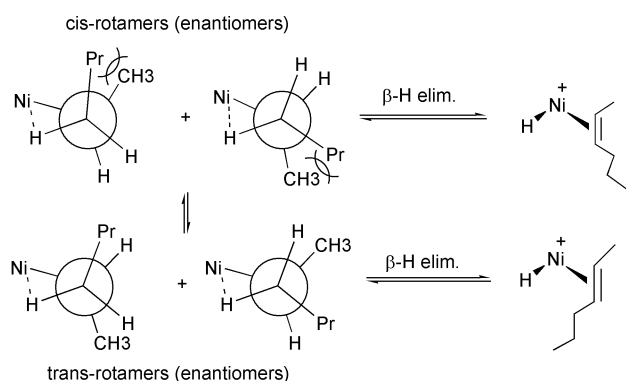

Scheme 2

Since an accurate analysis of the products revealed the absence of branched olefins in all reaction mixtures, the secondary alkyl–nickel compounds with the chelating diphos-

phines investigated do not undergo chain propagation, while they are apparently responsible for the formation of internal olefins. In this respect, the behaviour of the present chelating diphosphines diverges from that of Ni–α-diimines,[2] Ni–1,2-diiminophosphoranes[5] or sp²-hybridised phosphorus ligands such as 1,4-diphospha-1,3-butadienes,[6b] which commonly produce branching.

Studies on alkyl palladium–α-diimine complexes by Brookhart show that secondary metal–alkyl species may β-eliminate through β-agostic conformers of the type shown in Scheme 3,[19a] which illustrates the possible situation for the hexen-2-yl group bound to any Ni(P–P) system here investigated. Considering the rotamers shown in Scheme 3, one may suggest that the much larger production of *E*-internal olefins compared to *Z*-internal olefins (*vide infra*) is controlled by steric properties: indeed, the formation of the *cis*-rotamers, precursors to *Z*-hex-2-ene or *Z*-hex-3-ene, would be disfavoured over that of the *trans*-rotamers, precursors to *E*-isomers, due to the repulsion between the terminal alkyl groups.

Scheme 3

Steric and conformational effects seem to be extremely important also to differentiate the catalytic activity of the precursors **1**, **2**, **3** and **4**. The five-membered metalla-ring formed by *cyclo*-tetraphos is the most rigid in the series and the only one bearing two axial and two equatorial phenyl groups in both the solid state and solution. Therefore: (i) any β-H elimination process in the Ni(alkyl)(*cyclo*-tetraphos) fragment should be less facile than at any other Ni(alkyl)(P–P) fragment; (ii) any square-planar Ni-*cyclo*-tetraphos species during the catalysis will have at least one axial position sterically congested. As a consequence, termination *via* β-H transfer to the metal, involving a five-coordinate transition state, should be less favoured for *cyclo*-tetraphos complexes than for *meso*-dppb, *rac*-dppb and dppe complexes (Scheme 1).[19b] Consistent with decreasing ligand rigidity, the oligomerisation TOF has been found to decrease in the order **1** > **3** > **2** > **4**. On the other hand, the existence of a direct correlation between polymerisation activity and rigidity of the (chelating ligand)metal assembly/ligand steric bulk has been unequivocally established in a number of cases.[1a,5,9b,10,19]

The excellent stability of the catalyst generated by **1**/MAO, higher than that of any other catalyst examined, deserves a comment apart. Previous studies on palladium complexes have shown that ligand rigidity and ligand bulk contribute to stabilise (P–P)Pd–H moieties with respect to either proton loss, with formation of inactive Pd⁰ species, or to the formation of catalytically inactive (or less active) bis-chelate and binuclear compounds (P–P = chelating diphosphine, including those investigated here).[21] At the present stage where no information is available on the nature of (P–P)Ni–H species derived from **1–4**, the use of this concept to explain the remarkable stability of the *cyclo*-tetraphos catalyst would be highly speculative, yet rather realistic.

Conclusions

The presence of a rigid and planar cyclobutane backbone makes *cyclo*-tetraphos an excellent ligand to generate, in conjunction with NiCl₂ and MAO, a robust and active catalyst for the oligomerisation of ethylene to Schulz–Flory distributions of C_4–C_{14} olefins. Both chain transfer and chain propagation are first order in ethylene, which does not allow one to discriminate between termination by β-H transfer to nickel and termination by β-H transfer to monomer. However, the extensive isomerisation of α-olefins to internal olefins indicates the occurrence of β-H transfer to nickel. Diphosphines with a more flexible carbon backbone, such as *meso*-dppb, *rac*-dppb and dppe, form less active and less robust nickel catalysts, yielding prevalently butenes.

Experimental

General information

All reactions and manipulations were carried out under an atmosphere of nitrogen using Schlenk-type techniques. Dichloromethane was distilled from CaH₂. Reagent grade toluene, diethyl ether and *n*-pentane were freshly distilled from Na/benzophenone. All the other reagents and solvents were used as purchased from Aldrich, Fluka or Strem. The ligand 1,2 bis(diphenylphosphino)ethane (dppe), was used as purchased from Fluka or Strem. The ligands *meso*-2,3-bis(diphenylphosphino)butane (*meso*-2,3-dppb),[20b] *rac*-2,3-bis(diphenylphosphino)butane (*rac*-2,3-dppb),[20b] *cis,trans,cis*-1,2,3,4-tetrakis-(diphenylphosphino)cyclobutane (*cyclo*-tetraphos)[21] were prepared following literature methods. The complex NiCl₂(dppe) (**4**) was prepared as reported in the literature.[14a,b] All the isolated compounds and metal complexes were collected on sintered-glass frits and washed with appropriate solvents before being dried in a stream of nitrogen. Oligomerisation reactions were performed with a 500 mL stainless steel autoclave, constructed at the ICCOM-CNR (Firenze, Italy), equipped with a magnetic drive stirrer, a Parr 4842 temperature and pressure controller. The autoclave was connected to a gas reservoir to maintain a constant pressure all over the catalytic reactions. Deuterated solvents for NMR measurements were dried over molecular sieves. ¹H, and ³¹P{¹H} NMR spectra were obtained on either a Bruker ACP 200 (200.13 and 81.01 MHz, respectively). All chemical shifts are reported in ppm (δ) relative to tetramethylsilane, referenced to the chemical shifts of residual solvent resonances (¹H) or 85% H₃PO₄ (³¹P). Elemental analyses were performed using a Carlo Erba Model 1106 elemental analyzer. GC analyses were performed on a Shimadzu GC-14 A gas chromatographer equipped with a flame ionisation detector and a 30 m (0.25 mm i.d., 0.25 μm film thickness) SPB-1 Supelco fused silica capillary column using *n*-heptane as the external standard. GC/MS analyses were performed on a Shimadzu QP 5000 apparatus equipped with a column identical with that used for GC analysis. A Perkin-Elmer 8320GC equipped with a capillary column Al₂O₃/Na₂SO₄ PLOT Chrompack (length: 50 m, diameter 0.45 mm) was used to determine the isomeric composition of the hexene fractions.

Syntheses

The complexes Ni₂Cl₄(*cyclo*-tetraphos) (**1**), NiCl₂(*meso*-dppb) (**2**) and NiCl₂(*rac*-dppb) (**3**) were prepared through the following general procedure: 0.38 mmol of the ligand were dissolved in 20 mL of degassed CH₂Cl₂. To this solution were added 5 mL of degassed ethanol containing 0.76, 0.76 and 0.38 mmol of NiCl₂·6H₂O for the preparation of **1**, **2** and **3**, respectively. The solutions became immediately red. After stirring for 1.5 h at room temperature, the overall volume was reduced to about 10 mL. As a result, red–orange crystals precipitated. 15 mL of *n*-pentane were added to complete the separation of the metal

	1·2DMF	**2**·0.5toluene	**3**
Formula	$C_{58}H_{58}Cl_4N_2O_2P_4Ni_2$	$C_{31.5}H_{32}Cl_2P_2Ni$	$C_{28}H_{28}Cl_2P_2Ni$
FW	1198.20	602.12	556.05
Crystal system	Monoclinic	Monoclinic	Monoclinic
Space group	$P2(1)/n$	$P2(1)/n$	$P2(1)$
a/Å	12.018(2)	8.495(5)	7.7509 (1)
b/Å	18.891(4)	16.8561(15)	17.4206 (2)
c/Å	13.241(3)	20.561(6)	9.7140 (5)
β/°	108.53(3)	94.34(4)	102.218 (1)
T/K	293	293	243
Z	2	4	4
μ/mm^{-1}	1.002	0.971	1.105
Reflections, collected	6861	5303	11313
Reflections, unique	5713	5155	4411
R(int)	0.038	0.016	0.025
Final wR_2	0.1209 (3σ)	0.0952 (2σ)	0.0434 (2σ)
Final R	0.0595 (3σ)	0.0367 (2σ)	0.0165 (2σ)

complexes, which were filtered off, washed with 5 mL of *n*-pentane and dried in a stream of dry nitrogen. Yields: (**1**), 85%; (**2**), 84%; (**3**), 75%. Elemental analyses: (**1**) $C_{52}H_{44}Cl_4P_4Ni_2$: Calc. (%): C, 59.30; H, 4.18. Found (%): C, 59.01; H, 4.10. (**2**) $C_{28}H_{28}Cl_2P_2Ni$: Calc.: C, 60.48; H, 5.03. Found: C, 60.0; H, 5.00. (**3**) $C_{28}H_{28}Cl_2P_2Ni$: Calc.: C, 60.48; H, 5.03. Found: C, 60.40; H, 5.10.

(**1**) $^{31}P\{^1H\}$ NMR (DMF-d_7, 25 °C): δ = 72.52 (s); ^1H NMR (DMF-d_7, 25 °C): δ = 4.30 (br. s, 4H, C*H*P), 7.20–7.80 (m, 40H, C_6H_5).

(**2**) $^{31}P\{^1H\}$ NMR (CDCl$_3$, 25 °C): δ = 60.0 (s); ^1H NMR (CDCl$_3$, 25 °C): δ = 0.95 (dd, J_{PH} = 13.4 Hz, J_{HH} = 7.03 Hz, 6H, CHC*H$_3$*), 2.40 (m, 2H, C*H*CH$_3$), 7.35–8.25 (20H, C_6H_5); $^{31}P\{^1H\}$ NMR (CD$_2$Cl$_2$) at −78 °C : δ = 62.10 (d, J_{PP} = 79.2 Hz), 65.10 (d, J_{PP} = 79.2 Hz); ^1H NMR (CD$_2$Cl$_2$, −78 °C): δ = 0.75 (br. s, 3H, CHC*H$_3$*), 1.00 (br. s, 3H, CHC*H$_3$*), 2.60 (br. m, 2H, C*H*CH$_3$), 7.10–8.60 (m, 20H, C_6H_5). The slow exchange regime was attained at 195 K, while the coalescence temperature was determined at 221 K by $^{31}P\{^1H\}$ NMR spectroscopy.

(**3**) $^{31}P\{^1H\}$ NMR (CDCl$_3$, 25 °C): δ = 59.09 (s); ^1H NMR (CDCl$_3$, 25 °C): δ = 0.93 (dd, J_{PH} = 11.9 Hz, J_{HH} = 6.4 Hz, 6H, CHC*H$_3$*), 2.16 (m, 2H, C*H*CH$_3$), 7.45–8.45 (20H, C_6H_5).

X-Ray crystal structure determinations

Crystal parameters and other experimental details of data collections are summarised in Table 4. Well-shaped crystals of **1**·2DMF were obtained by evaporation of a saturated DMF solution of **1** at room temperature. All X-ray diffraction data were collected on a Siemens P4 diffractometer using ω-scans. Cell refinements and data reduction were done by the software of the Siemens P4 diffractometer,[22] and the empirical absorption corrections were based on ψ-scans of nine reflections, respectively (χ = 78–102°, 360° scans in 10° steps in ψ).[23] All structure determination calculations were carried out using SHELXTL NT 5.10 including SHELXS-97[24a] and SHELXL-97.[24b] Final refinements on F^2 were carried out with anisotropic thermal parameters for all non-hydrogen atoms. The hydrogen atoms were included using a riding model with isotropic U values depending on U_{eq} of the adjacent carbon atoms.

Crystals of **2** suitable for a X-ray analysis were obtained by slow evaporation of a CH$_2$Cl$_2$/toluene solution at room temperature. From the X-ray analysis it turned out that the asymmetric unit contains also a disordered toluene molecule. The data for this crystal structure were collected with an Enraf-Nonius CAD4 diffractometer. A set of 25 carefully centered reflections having $5.0° \leq \Theta \leq 11.0°$ were used to determine the lattice constants. The data were corrected for Lorentz and polarization effects. Atomic scattering factors with anomalous dispersion correction were taken from X-ray crystallography tables.[25a,b] Absorption correction was applied *via* ψ scans. The structure was solved by direct methods using

the SIR92 program,[26] and all of the non-hydrogen atoms were found through a series of F_0 Fourier maps. Refinement was done by full-matrix least-squares calculations, initially with isotropic thermal parameters and finally with anisotropic thermal parameters for all the atoms but the hydrogens. The phenyl rings were treated as rigid bodies with D_{6h} symmetry, and hydrogens were introduced at calculated positions.

Single crystals of **3** were obtained by evaporation of a saturated CH$_2$Cl$_2$/toluene solution at room temperature. All data were collected on a Nonius Kappa CCD diffractometer using combined ϕ–ω-scans. Cell refinement, data reduction, and the empirical absorption correction were done by Denzo and Scalepack programs.[27] All structure determination calculations were carried out using SHELXTL NT 5.10 including SHELXS-97[24a] and SHELXL-97.[24b] Final refinements on F^2 were carried out with anisotropic thermal parameters for all non-hydrogen atoms. The hydrogen atoms were included using a riding model with isotropic U values depending on U_{eq} of the adjacent carbon atoms. The Flack parameter of −0.011(9) clearly indicates the presence of the pure NiCl$_2$(R,R-2,3-dppb) enantiomer in the crystal.

CCDC reference numbers 215914, 218038 and 218039.

See http://www.rsc.org/suppdata/dt/b3/b308388h/ for crystallographic data in CIF or other electronic format.

Oligomerisation reactions

General procedure. A 500 mL stainless-steel reactor was heated at 60 °C under vacuum for 3 h and then cooled down to room temperature under vacuum. The solid precatalyst (12 μmol) was introduced into the autoclave at room temperature under a dinitrogen atmosphere, and the system was purged 4 times with nitrogen/vacuum cycles. A solution of 100 mL of oxygen-free toluene and 2.0 mL of MAO (toluene solution, 10 wt%) was then introduced into the reactor by suction. The autoclave was stirred at room temperature for 2 min at 1500 rpm, then it was filled with ethylene to the desired pressure and immediately stirred at 1500 rpm, maintaining a constant gas pressure with a gas reservoir. After the desired reaction time the autoclave was cooled down to 5 °C by means of an ice/acetone bath, slowly depressurised and the reaction was quenched by addition of 2 ml of MeOH acidified with dilute HCl. *n*-Heptane (200 μL) was finally introduced as internal standard for GC and GC/MS analysis.

Oligomerisation of ethylene in the presence of 1-undecene. A 0.5 L stainless-steel reactor was heated at 60 °C under vacuum for 3 h and then cooled down to room temperature under vacuum. Pre-catalyst **1** (12 μmol) was introduced into the autoclave at room temperature under a dinitrogen atmosphere, and the system was purged 4 times with nitrogen/vacuum cycles. A solution of 100 mL of oxygen-free toluene and 2.0 mL of

MAO (toluene solution, 10 wt%) was then introduced into the reactor by suction together with 0.5 mL (24.3 mmol) of 1-undecene. The reactor was then pressurized with ethylene (4 bar) and stirred (1500 rpm). After 30 min the autoclave was rapidly cooled to 5 °C, depressurized and the reaction was quenched by addition of 2 mL of MeOH. n-Heptane (200 µL) was finally introduced as internal standard for GC measurements. TOF 1.69×10^4 mol C_2H_4 converted (mol Ni × h)$^{-1}$; $a = 0.265$; no appreciable formation of odd oligomer ($C_{11 + 2n}$) was detected, while undecene isomerisation occurred to give internal isomers.

Acknowledgements

References

1 (a) W. Keim and R. P. Schulz, *J. Mol. Catal.*, 1994, **92**, 21; (b) D. Vogt, *Applied Homogeneous Catalysis with Organometallic Compounds*, ed. B. Cornils and W. A. Herrmann, Wiley, New York, 1998, p. 240.

2 (a) S. A. Sveida and M. Brookhart, *Organometallics*, 1999, **18**, 65; (b) C. M. Killian, L. K. Johnson and M. Brookhart, *Organometallics*, 1997, **16**, 2005; (c) S. Stroemberg, M. Ohsman, L. Zhang and K. Zetterberg, *Acta Chem. Scand.*, 1995, **49**, 689.

3 (a) P. L. Bress, V. C. Gibson, C. D. F. Mabille, W. Reed, D. F. Wass and R. H. Weatherhead (BP Chemicals Ltd), WO 98/49208, 1998; P. L. Bress, V. C. Gibson, C. D. F. Mabille, W. Reed, D. F. Wass and R. H. Weatherhead, *Chem. Abstr.*, 1999, **130**, 4185; (b) S. Plentz Meneghetti, P. J. Lutz and J. Kress, *Organometallics*, 1999, **18**, 2734; (c) T. V. Laine, K. Lappalainen, J. Liimatta, E. Aitola, B. Loefgren and M. Leskelae, *Macromol. Rapid Commun.*, 1999, **20**, 487; (d) T. V. Laine, M. Klinga, A. Maainen and E. Aitola, *Acta Chem. Scand.*, 1999, **53**, 968.

4 E. K. van den Beuken, W. J. J. Smeets, A. L. Spek and B. L. Feringa, *Chem. Commun.*, 1998, 223.

5 M. Sauthier, F. Leca, R. F. de Souza, K. B. Gusmaa, L. F. Trevisab Queiroz, L. Toupet and R. Rèau, *New J. Chem.*, 2002, **26**, 630.

6 (a) O. Daugulis, M. Brookhart and P. S. White, *Organometallics*, 2002, **21**, 5935; (b) A. Jonkin and W. Marshall, *Chem. Commun.*, 2003, 710; (c) S. Ikeda, F. Okhata, M. Miyoshi, R. Tanaka, T. Minami, F. Ozawa and M. Yoshifuji, *Angew. Chem., Int. Ed.*, 2000, **39**, 4512.

7 S. Y. Desjardins, A. A. Way, M. C. Murray, D. Adirim and M. C. Baird, *Organometallics*, 1998, **17**, 2382.

8 (a) H. D. Mui, M. E. Riehl, S. R. Wilson and G. S. Girolami, *ACS Abstr.,* **208**(part 1), 530; (b) A. Hoehn, F. Lippert and E. Schauss (BASF), WO96/37522, 1996; (c) M. Brookhart, J. Feldman, E. Hauptman, and E. F. Mc Cord (DuPont), WO 98/47934, 1998.

9 (a) N. A. Cooley, S. M. Green and D. F. Wass, *Organometallics*, 2001, **20**, 4769; (b) A. Carter, N. A. Cooley, P. G. Pringle, J. Scutt and D. F. Wass, *Polym. Mater. Sci. Eng.*, 2002, **86**, 314; (c) W. Keim, R. Appel, S. Gruppe and F. Knoch, *Angew. Chem., Int. Ed.*, 1987, **26**, 1012.

10 C. Bianchini, H. M. Lee, A. Meli, W. Oberhauser, F. Vizza, P. Brueggeller, R. Haid and C. Langes, *Chem. Commun.*, 2000, 777.

11 C. Bianchini, G. Mantovani, A. Meli, W. Oberhauser, P. Brueggeller and T. Stampfl, *J. Chem. Soc., Dalton Trans.*, 2001, 690.

12 (a) *Principles and Application of Organotransition Metal Chemistry*, ed. J. P. Collman, L. Hegedus, J. R. Norton and R. G. Finke, University Science Books, Mill Valley, CA, 1987, p. 386; (b) P. Margl and T. Ziegler, *J. Am. Chem. Soc.*, 1996, **118**, 7337.

13 (a) R. Busby, M. B. Hursthouse, P. S. Jarrett, C. W. Lehmann, K. M. Abdul Malik and C. Phillips, *J. Chem. Soc., Dalton Trans.*, 1993, 3767; (b) S. C. Davies, R. A. Henderson, D. L. Hughes and K. E. Oglieve, *J. Chem. Soc., Dalton Trans.*, 1998, 425.

14 (a) P. A. MacNeil, N. K. Roberts and B. Bosnich, *J. Am. Chem. Soc.*, 1981, **103**, 2273; (b) M. D. Fryzuk and B. Bosnich, *J. Am. Chem. Soc.*, 1977, **99**, 6262.

15 (a) J. Bakos, I. Toth, B. Heil, G. Szalontai, L. Pàrkànyi and V. Fuelop, *J. Organomet. Chem.*, 1989, **370**, 263; (b) W. N. Rahmouni, J. A. Osborne, A. De Cian, J. Fischer and A. Ezzamarty, *Organometallics*, 1998, **17**, 2470; (c) L. Gonsalvi, H. Adams, G. J. Sunley, E. Ditzel and A. Haynes, *J. Am. Chem. Soc.*, 2002, **124**, 13597.

16 (a) P. J. Flory, *J. Am. Chem. Soc.*, 1940, **62**, 1561; (b) G. V. Schulz, *Z. Phys. Chem., B*, 1935, **30**, 379; (c) G. V. Schulz, *Z. Phys. Chem., B*, 1939, **43**, 25.

17 (a) B. L. Small and M. Brookhart, *J. Am. Chem. Soc.*, 1998, **120**, 7143; (b) G. J. P. Britovsek, S. Mastroianni, G. A. Solan, S. P. D. Baugh, C. Redshaw, V. C. Gibson, A. J. P. White, D. J. Williams and M. R. J. Elsegood, *Chem. Eur. J.*, 2000, **6**, 2221; (c) C. Bianchini, G. Mantovani, A. Meli, F. Migliacci, F. Zanobini, F. Laschi and A. Sommazzi, *Eur. J. Inorg. Chem.*, 2003, 1620; (d) C. Bianchini, G. Mantovani, A. Meli, F. Migliacci and F. Laschi, *Organometallics*, 2003, **22**, 2545.

18 (a) B. L. Small, M. Brookart and A. M. A. Bennett, *J. Am. Chem. Soc.*, 1998, **120**, 4049; (b) G. J. P. Britovsek, V. C. Gibson, B. S. Kimberley, P. J. Maddox, S. J. McTavish, G. A. Solan, A. J. P. White and D. J. Williams, *Chem. Commun.*, 1998, 849; (c) G. J. P. Britovsek, M. Bruce, V. C. Gibson, B. S. Kimberley, P. J. Maddox, S. Mastroianni, S. J. McTavish, C. Redshaw, G. A. Solan, S. Stromberg, A. J. P. White and D. J. Williams, *J. Am. Chem. Soc.*, 1999, **121**, 8728; (d) F. A. R. Kaul, G. T. Puchta, H. Schneider, F. Bielert, D. Mihalios and W. A. Herrmann, *Organometallics*, 2002, **21**, 74.

19 (a) L. H. Schultz, D. J. Tempel and M. Brookhart, *J. Am. Chem. Soc.*, 2001, **123**, 11539; (b) S. D. Ittel, L. K. Johnson and M. Brookhart, *Chem. Rev.*, 2000, **100**, 1169.

20 (a) C. Bianchini and A. Meli, *Coord. Chem. Rev.*, 2002, **225**, 35; (b) C. Bianchini, H. M. Lee, A. Meli, W. Oberhauser, M. Peruzzini and F. Vizza, *Organometallics*, 2002, **21**, 16; (c) C. Bianchini, A. Meli, G. Mueller, W. Oberhauser and E. Passaglia, *Organometallics*, 2002, **21**, 4965.

21 W. Oberhauser, C. Bachmann, T. Stampfl, R. Haid, C. Langes, H. Kopacka, A. Rieder and P. Brueggeller, *Inorg. Chim. Acta*, 1999, **290**, 167.

22 SHELXTL Version 4.2, Siemens Analytical X-Ray Instruments, Madison, WI, 1991.

23 A. C. T. North, D. C. Phillips and F. S. Mathews, *Acta Crystallogr., Sect. A*, 1968, **24**, 351.

24 (a) G. M. Sheldrick, *Acta Crystallogr., Sect. A*, 1990, **46**, 467; (b) G. M. Sheldrick, SHELXL-97, Program for refinement of crystal structures, University of Göttingen, Germany, 1997.

25 (a) A. J. Wilson, *International Tables for X-Ray Crystallography*, Kluwer, Dordrecht, The Netherlands, 1992, p. 219; (b) A. J. Wilson, *International Tables for X-Ray Crystallography*, Kluwer, Dordrecht, The Netherlands, 1992, p. 500.

26 A. Altomare, G. Cascarano, C. Giacovazzo, A. Gagliardi, M. C. Burla, G. Polidori and M. Cavalli, *J. Appl. Crystallogr.*, 1994, **27**, 435.

27 Z. Otwinowski and W. Minor, in *Methods in Enzymology*, vol. 276, *Macromolecular Crystallography, Part A*, ed. C. W. Carter and R. W. Sweet, Academic Press, New York, 1997, p. 307.